

This document is the Accepted Manuscript version of a Published Work that appeared in final form in Journal of Organic Chemistry, copyright © American Chemical Society after peer review and technical editing by the publisher.

To access the final edited and published work see <https://doi.org/10.1021/acs.joc.9b00462>

This Accepted Manuscript version of a Published Work is available from <https://hdl.handle.net/10195/74918>



This postprint version is licenced under a [Creative Commons Attribution-NonCommercial-NoDerivatives 4.0 International](https://creativecommons.org/licenses/by-nc-nd/4.0/).

Article

## C–H Functionalizations by Palladium Carboxylates: The Acid Effect

Jiri Vana, Jan Bartacek, Jiri Hanusek, Jana Roithová, and Milos Sedlak

*J. Org. Chem.*, **Just Accepted Manuscript** • DOI: 10.1021/acs.joc.9b00462 • Publication Date (Web): 29 Mar 2019

Downloaded from <http://pubs.acs.org> on April 2, 2019

### Just Accepted

“Just Accepted” manuscripts have been peer-reviewed and accepted for publication. They are posted online prior to technical editing, formatting for publication and author proofing. The American Chemical Society provides “Just Accepted” as a service to the research community to expedite the dissemination of scientific material as soon as possible after acceptance. “Just Accepted” manuscripts appear in full in PDF format accompanied by an HTML abstract. “Just Accepted” manuscripts have been fully peer reviewed, but should not be considered the official version of record. They are citable by the Digital Object Identifier (DOI®). “Just Accepted” is an optional service offered to authors. Therefore, the “Just Accepted” Web site may not include all articles that will be published in the journal. After a manuscript is technically edited and formatted, it will be removed from the “Just Accepted” Web site and published as an ASAP article. Note that technical editing may introduce minor changes to the manuscript text and/or graphics which could affect content, and all legal disclaimers and ethical guidelines that apply to the journal pertain. ACS cannot be held responsible for errors or consequences arising from the use of information contained in these “Just Accepted” manuscripts.



ACS Publications

is published by the American Chemical Society, 1155 Sixteenth Street N.W.,  
Washington, DC 20036

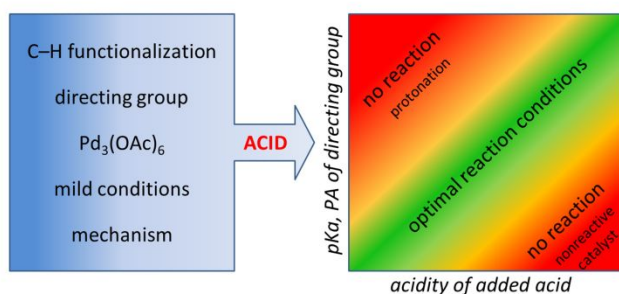
Published by American Chemical Society. Copyright © American Chemical Society.  
However, no copyright claim is made to original U.S. Government works, or works  
produced by employees of any Commonwealth realm Crown government in the course  
of their duties.

# C–H Functionalizations by Palladium Carboxylates: The Acid Effect

Jiří Váňa,<sup>\*,†</sup> Jan Bartáček,<sup>†</sup> Jiří Hanusek,<sup>†</sup> Jana Roithová<sup>‡</sup> and Miloš Sedláč<sup>†</sup>

<sup>†</sup>Institute of Organic Chemistry and Technology, Faculty of Chemical Technology,  
University of Pardubice, Studentská 573, 53210 Pardubice, The Czech Republic

<sup>‡</sup>Department for Spectroscopy and Catalysis, Institute for Molecules and Materials  
Radboud University, Heyendaalseweg 135, 6525 AJ Nijmegen, The Netherlands



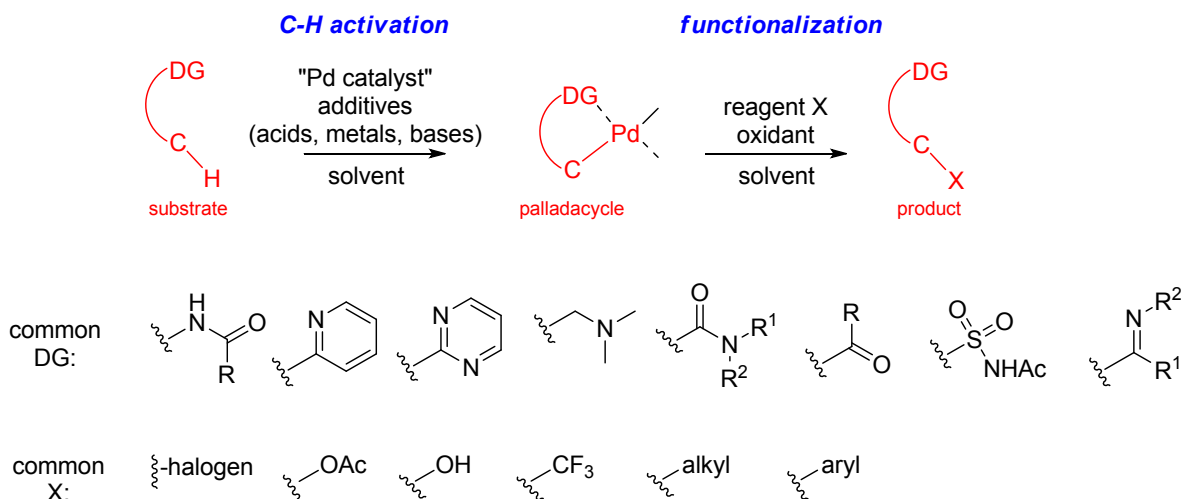
**KEYWORDS** C–H activation, cyclopalladation, C–H functionalization, reaction mechanism, carboxylic acids, DFT calculations

1  
2  
3  
4  
5  
6  
7 ABSTRACT Finding optimal reaction conditions is usually complex, requires many  
8  
9  
10 experiments and is therefore demanding in terms of human, financial and environmental  
11  
12  
13 resources. This work provides a simple workflow for easier design of popular palladium  
14  
15  
16 catalyzed C–H functionalization reactions, where the active palladium catalysts contain  
17  
18  
19 carboxylate ligands. The key factor for optimizing reaction conditions is to find a balance  
20  
21  
22 between two opposing effects of the carboxylic acid in the reaction mixture; generation  
23  
24  
25 of more reactive palladium catalyst *vs.* deactivation of substrate by its protonation.  
26  
27  
28  
29  
30  
31  
32  
33

## 34 INTRODUCTION

35  
36  
37  
38 Palladium catalyzed C–H functionalization reactions controlled by directing groups  
39  
40  
41 (DG) are used for facile approach to compounds with new C–C and C–heteroatom  
42  
43  
44 bonds<sup>1</sup> (Scheme 1) that find application as organic intermediates, pharmaceuticals,  
45  
46  
47 agrochemicals or natural products analogues.<sup>2</sup> While this reaction has a broad  
48  
49  
50 application scope, the optimal reaction conditions can vary substantially. Therefore,  
51  
52  
53 researchers optimize reaction conditions for each individual system. However, the  
54  
55  
56  
57  
58  
59  
60

1  
2  
3 complexity of the reaction mixtures and incomplete understanding of the reaction  
4  
5  
6  
7 mechanism often make the search for optimal reaction conditions a rather elaborate  
8  
9  
10 pursuit. A more efficient way is to design reaction conditions based on the given  
11  
12  
13 reaction mechanism and recognition of the effects of the individual reaction components  
14  
15  
16  
17 on this mechanism.  
18  
19  
20  
21  
22  
23  
24  
25  
26  
27  
28  
29  
30  
31  
32  
33  
34  
35  
36  
37  
38  
39  
40  
41  
42  
43  
44  
45  
46  
47  
48  
49  
50  
51  
52  
53  
54  
55  
56  
57  
58  
59  
60

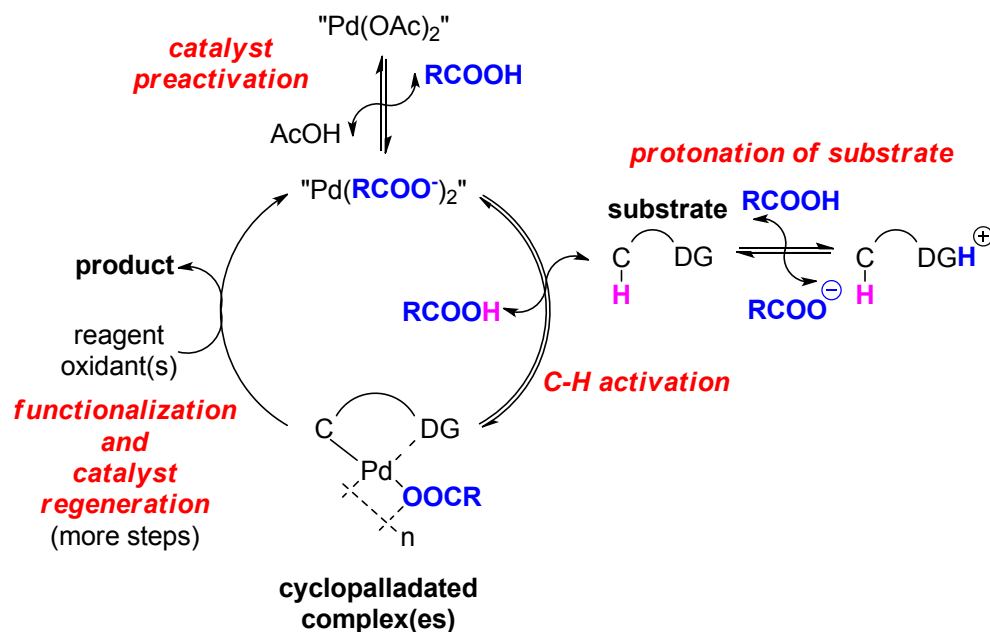


23 **Scheme 1.** General scheme for the transition metal assisted C–H functionalization  
24 reactions showing examples of typical directing (DG) and functionalizing groups (X).  
25  
26  
27

28  
29 In general, catalytic C–H functionalization consists of several main steps.<sup>3</sup> First, the  
30 formation of a precatalyst, where palladium catalyst reacts with additives (mainly acids  
31 or other metal salts) to give the catalytically active species. Second, the C–H activation  
32 step where a directing group brings palladium to the proximity of the given C–H bond  
33 and subsequently the hydrogen atom is substituted for palladium *via* concerted  
34 metalation–deprotonation (CMD) transition state. This leads to the formation of  
35 palladacycles mainly existing in monomeric or dimeric forms, although polynuclear  
36 species were observed, too.<sup>4</sup> In the third (multiple) step, the reaction of palladacycle  
37  
38  
39  
40  
41  
42  
43  
44  
45  
46  
47  
48  
49  
50  
51  
52  
53  
54  
55  
56  
57  
58  
59  
60

1  
2  
3 with a reagent leads to the formation of the product. Finally, the palladium precatalyst is  
4  
5  
6  
7 regenerated and enters into a new catalytic cycle.  
8  
9

10 In principle, each reaction component is primarily intended to be responsible for one  
11  
12  
13  
14 reaction step. However, it can affect other reaction steps, too. Until now, there has been  
15  
16  
17  
18 no all-embracing study on how reaction components affect palladium promoted C–H  
19  
20  
21 functionalizations. However, some dedicated reactivity studies do exist. For example,  
22  
23  
24 Sanford<sup>5</sup> investigated effects of the directing groups in C–H bond functionalization.  
25  
26  
27  
28 Several groups investigated the effect of added substituted acetic<sup>6</sup> or benzoic acids<sup>7</sup> on  
29  
30  
31  
32 functionalization efficiency. Finally, much theoretical work exists to rationalize the  
33  
34  
35  
36 reaction mechanisms of carboxylate assisted C–H functionalization as Davies recently  
37  
38 summarized.<sup>8</sup>  
39  
40  
41  
42  
43  
44  
45  
46  
47  
48  
49  
50  
51  
52  
53  
54  
55  
56  
57  
58  
59  
60



**Scheme 2.** Simplified scheme for the palladium carboxylates catalyzed directing group assisted C–H functionalization reactions showing potential places of action of added carboxylic acids.

Deeper insight into the typical reaction scheme (Scheme 2) suggests that added carboxylic acids are the key factor for reactivity control. These acids may influence reaction by at least five different ways: (1) form a precatalyst from palladium acetate; (2) affect the reactivity of palladium in the C–H activation step; (3) protonate substrate; (4) affect oxidation potentials of palladacycles and thus their reactivity in functionalization step;<sup>9</sup> (5) exchange anions in other common reagents; e.g.,  $\text{PhI(OAc)}_2$  or  $\text{Cu(OAc)}_2$ .



1  
2  
3 Here, we are going to show the effect of added carboxylic acids on key reaction steps  
4  
5  
6  
7 and how these findings can be used for simplifying of reaction conditions screening and  
8  
9  
10 for facilitating reactions under milder conditions.  
11  
12  
13  
14  
15  
16

## 17 RESULTS AND DISCUSSION

18  
19  
20

### 21 *Effect of carboxylic acids on rate of precatalyst formation*

22  
23

24 As was shown in our previous work,<sup>10</sup> addition of trifluoroacetic acid (TFA) to the  
25  
26  
27 Pd<sub>3</sub>(OAc)<sub>6</sub> causes sequential exchange of acetate for trifluoroacetate ligands leading to  
28  
29  
30 more reactive Pd<sub>3</sub>(TFA)<sub>6</sub>. This preactivation step is necessary for the C–H activation of  
31  
32  
33 acetanilides and is completed within few minutes. In the next series of <sup>1</sup>H NMR kinetic  
34  
35  
36 experiments, we examined the influence of acid strength on the exchange rate (Fig.  
37  
38  
39 S1). We compared rates of the ligand exchange for five different carboxylic acids:  
40  
41  
42 trifluoroacetic (pK<sub>a</sub> -0.26, ( $\Delta PA_{exp}$  25.8),<sup>11,12</sup> trichloroacetic (pK<sub>a</sub> 0.77), dichloroacetic  
43  
44  
45 (pK<sub>a</sub> 1.29,  $\Delta PA_{exp}$  20.3), chloroacetic (pK<sub>a</sub> 2.86,  $\Delta PA_{exp}$  12.4) and tetradeuteroacetic.  
46  
47  
48  
49  
50  
51  
52 The half-lives for the individual exchanges are summed in Table 1. Comparison of the  
53  
54  
55  
56 results shows that the rate of ligand exchange increases with acidity of carboxylic acid  
57  
58  
59  
60

and is in good correlation with proton affinity ( $\Delta PA_{exp}$ ) values. Especially in the case of weaker acids the catalyst preactivation can be a kinetically significant step.

**Table 1.** Physical constants of substituted carboxylic acids and measured half-lives of the exchange of acetate ligands in  $Pd_3(OAc)_6$  for different carboxylate ligands.

Acid	pKa	$\Delta PA_{exp}$	$\Delta H_D^{0\ 13}$	$t_{1/2}$ (s) <sup>a</sup>
TFA	-0.26	25.8	322.7	16
trichloroacetic	0.77			15
dichloroacetic	1.29	20.3	328.4	30
chloroacetic	2.86	12.4	335.4	91
methoxyacetic	3.53	6.6	341.9	
Ac-Val-OH	$\approx 3.7^b$			
acetic	4.76	0	348.5	
CD <sub>3</sub> COOD				304

<sup>a</sup>The values are obtained from <sup>1</sup>H NMR monitoring of decrease of overall amount of acetate ligands coordinated to palladium.

<sup>b</sup>Value is expected to be in a similar range as Ac-Gly-OH ( $pK_a = 3.67$ ) and Ac-Ala-OH ( $pK_a = 3.70$ ).<sup>14</sup>

### *Effect of acids on reactivity of starting material*

Carboxylic acids in reaction mixture can strongly affect reactivity of substrates by protonation. Shi and coworkers showed that *N,N*-dimethylbenzylamines (DMBA) can be C-H activated in the presence of a suitable amount of acetic acid. However, in the presence of more acidic TFA the reaction does not occur.<sup>6a</sup> We studied this effect by NMR titration of different substrates by various carboxylic acids (Figures S1-5). Very illustrative is the comparison of shapes of titration curves in the case of titration of *N,N*-dimethylbenzylamine ( $pK_a \approx 9$ ) with acetic, dichloroacetic and trifluoroacetic acids (Fig. 2). The titration curves show that in the case of strong trifluoroacetic and dichloroacetic acids the break occurs at acid/DMBA ratio = 1. This means that *N,N*-dimethylbenzylamine is fully protonated after addition of 1 equivalent of acid. Full protonation is further confirmed by the shapes of NMR signals of CH<sub>2</sub> and CH<sub>3</sub> groups of *N,N*-dimethylbenzylamine. These signals change from singlets at the beginning of the titration to doublets after protonation (see inset in Figure 1). Contrary to this, titration

curve obtained for acetic acid is relatively smooth without any sharp break, thus indicating a weaker association.

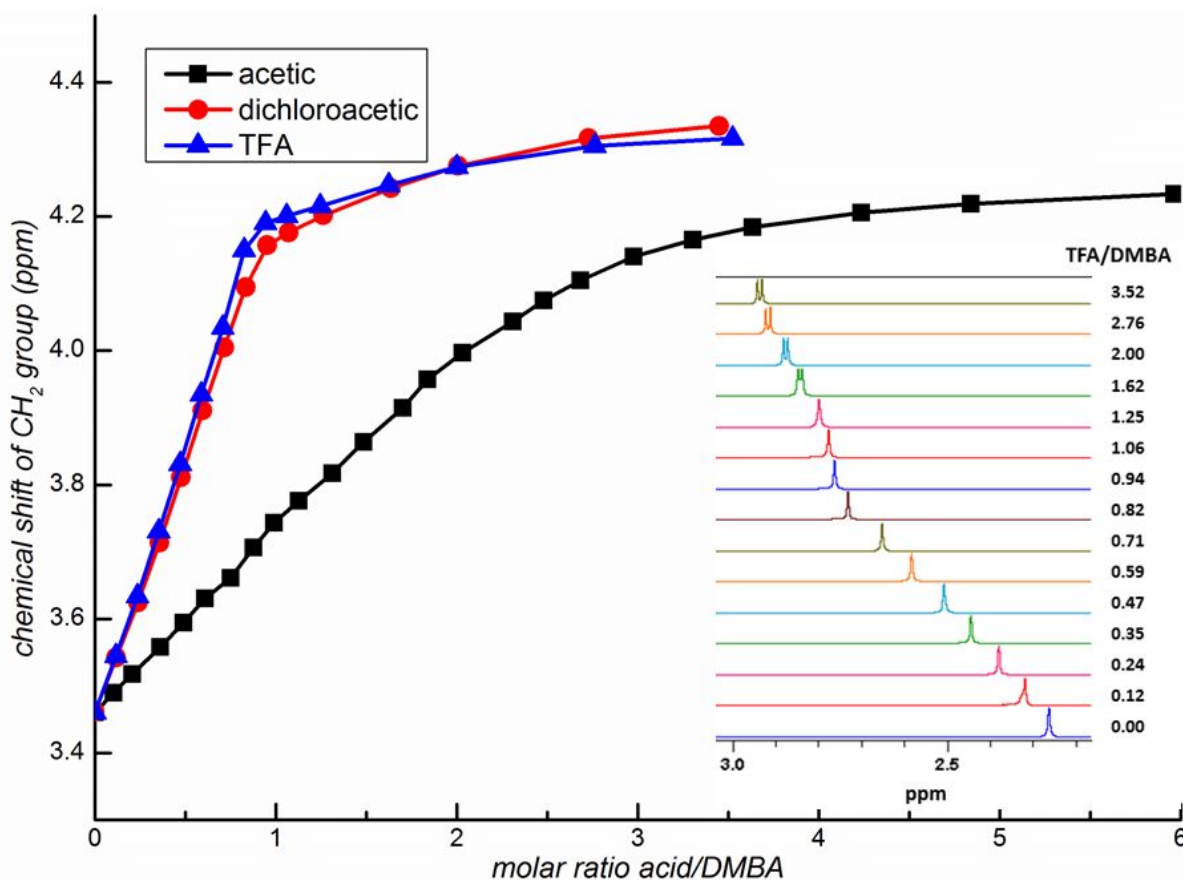


**Figure 1.** Changes of  $^1\text{H}$  NMR chemical shifts of benzylic protons caused by titration of *N,N*-dimethylbenzylamine (DMBA) by acetic (black squares), dichloroacetic (red circles) and trifluoroacetic (TFA) (blue triangles) acids in  $\text{CD}_2\text{Cl}_2$ . Inset shows changes in chemical shifts and signal shapes in the case of titration by TFA.

To quantify the measured data, we fitted the titration curves using BindFit software.<sup>15</sup>

The best match was obtained for substrate/acid ratio 1:2 (Figures. S6-14). The

calculated association constants are summarized in Table 2 and in more detail in Table S1. The data reveal a strong association between the most basic DMBA and stronger acids (TFA and dichloroacetic). In the case of 2-phenylpyridine (Ph-Py) ( $pK_a \approx 4.4$ ), the stronger association is observed only in the case of TFA. Finally, there is no strong association in the case of 3-bromoacetanilide (3-Br-acetanilide) ( $pK_a \approx -4.4$ ). These data illustrate why DMBA is non-reactive in reaction mixtures containing strong acids. More importantly, it can be concluded that addition of a too strong acid to the reaction mixture causes protonation of the substrate and thus retardation of the reaction.

**Table 2.** Values of first association constants obtained from NMR titrations by BindFit software.

	DMBA	Ph-Py	3-Br-acetanilide
Acid	$K_{1,1}$ ( $M^{-1}$ )	$K_{1,1}$ ( $M^{-1}$ )	$K_{1,1}$ ( $M^{-1}$ )
acetic	$0.67 \pm 0.03$	$10 \pm 1$	$6 \pm 2$
dichloroacetic	$238 \pm 89$	$55 \pm 8$	$16 \pm 2$
TFA	$424 \pm 361$	$975 \pm 585$	$10 \pm 1$

### *Influence of added acids on C–H activation step*

The DFT calculations provide a view on the detailed mechanism of the C–H activation reaction and illustrate the effect of the additional acids on the reactivity of the palladium catalyst. Here we report reaction profiles for two substrates located at the opposite sides of the acidity scale; acetanilide ( $pK_a \approx -4.4$ ) and *N,N*-dimethylbenzylamine ( $pK_a \approx 9$ ). For simplification, both models are based on mono-palladium species. However, the reactivity trends should remain identical in the case of polynuclear species that were proposed to be the key species in some cases.<sup>4</sup>

The C–H activation of acetanilide (Fig. 2) begins with *O*-coordinated complex **1**.<sup>16</sup> The first reaction step is an electrophilic attack of palladium cation at the aromatic system and formation of  $\pi$ -complex **2**. Then, palladium slips to the *ortho* position of acetanilide to form  $\sigma$ -complex **3**. Next, proton is transferred *via* agostic TS to form palladacycle **4**. This further conformationally relaxes to give palladacycle **5**. The effect of different basicity of carboxylate ligands is illustrated in Figure 2.

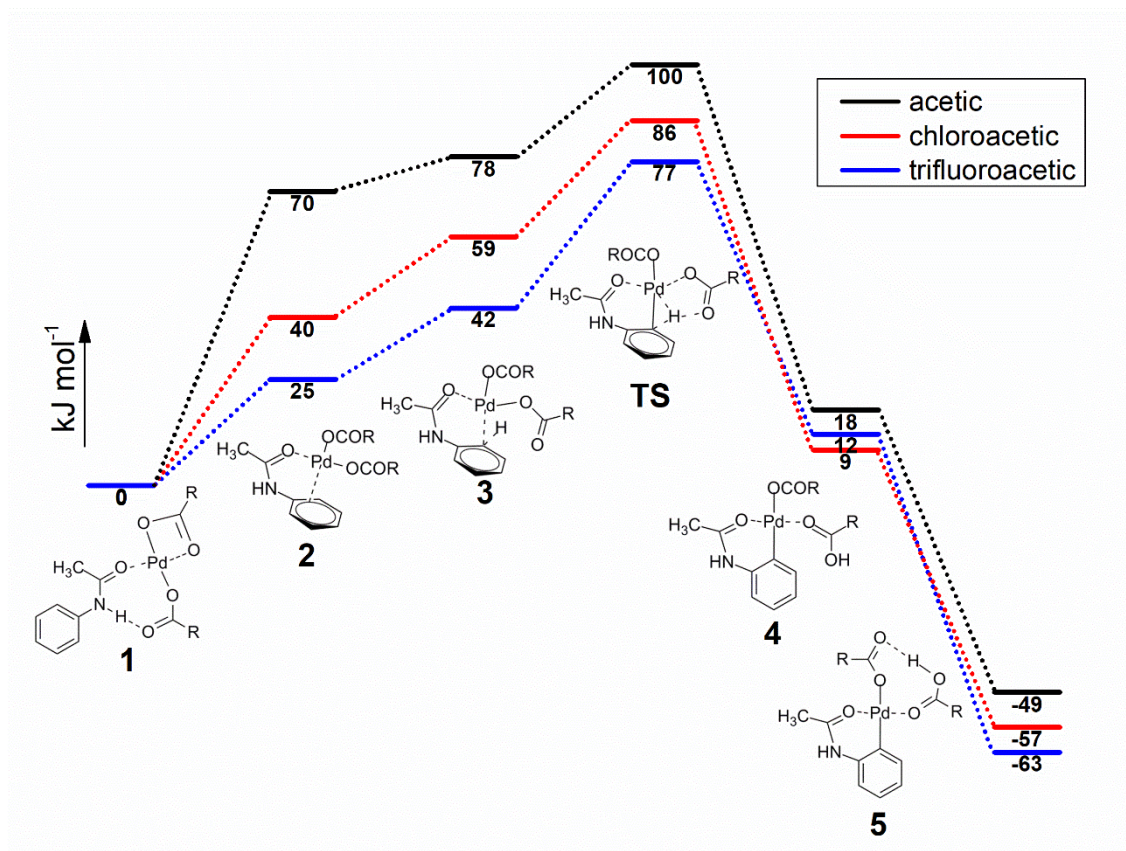


**Figure 2.** Reaction profile (relative Gibbs energies in DCM at 298 K in  $\text{kJ mol}^{-1}$ ) of C–H activation step calculated for reaction of acetanilide with palladium acetate (black), chloroacetate (red) and trifluoroacetate (blue).

The carboxylate ligand is an electron acceptor and therefore makes palladium more electrophilic.<sup>17</sup> The calculated NPA charges on Pd in monomeric palladium(II) carboxylates are growing in order 0.385 (acetate) 0.392 (chloroacetate) 0.405 (trifluoroacetate). The more electron-withdrawing carboxylate ligands facilitate formation of the  $\pi$ - and  $\sigma$ -complexes and thus make the pathway towards C–H activation more

1  
2  
3 energy accessible (cf. Figure 2). At the same time, the more electron-withdrawing  
4  
5  
6  
7 carboxylate ligand stabilizes better the organopalladium product and makes the C–H  
8  
9  
10 activation step more exothermic. Hence overall, the calculations suggest that  
11  
12  
13  
14 carboxylate ligands formed from stronger acids favor the C–H activation reactions  
15  
16  
17 kinetically as well as thermodynamically.  
18  
19  
20

21       On the other hand, the larger basicity of less electron-withdrawing carboxylate ligand  
22  
23  
24 make the elementary hydrogen atom transfer from carbon to oxygen more exothermic  
25  
26  
27 (step 3 → 4). The key interatomic distances in transition structures obtained with  
28  
29  
30  
31 different carboxylate ligands nicely illustrate this effect. The less electron-withdrawing  
32  
33  
34  
35 carboxylate ligands favor early transition structures with geometries closer to the  
36  
37  
38  $\sigma$ -complexes (Figure 3). Conversely, the more electron withdrawing ligands favor late  
39  
40  
41  
42 transition structures with more developed O–H and Pd–C bonds.  
43  
44  
45  
46  
47  
48  
49  
50  
51  
52  
53  
54  
55  
56  
57  
58  
59  
60



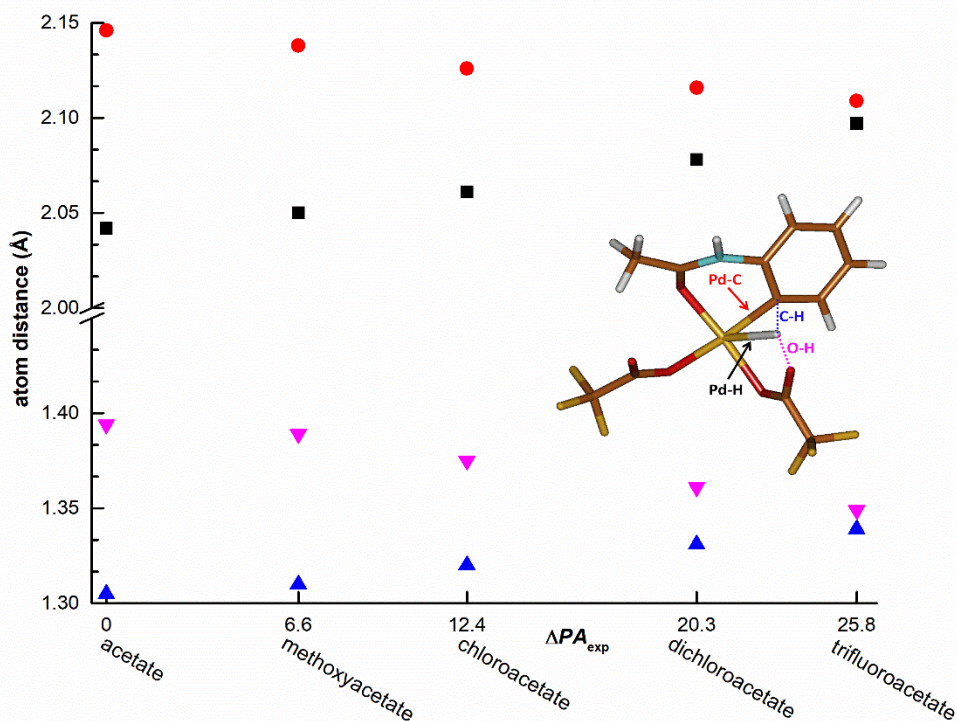


**Figure 3.** Important atom distances Pd–H (black squares); Pd–C (red circles); C–H (blue triangles); O–H (violet triangles) in agostic transition states calculated with different carboxylate ligands in dependence on  $\Delta PA_{exp}$ .

Reaction profiles and atom distances calculated for C–H activation of *N,N*-dimethylbenzylamine (Figure S15) show the very same trends as the results for acetanilide.<sup>18</sup> In summary, DFT calculations show that addition of stronger acids to the reaction system facilitates the C–H activation step both, kinetically and thermodynamically. The effect is caused by increased electrophilicity of palladium atom.

1  
2  
3  
4  
5  
6  
7 *Kinetics of C–H activation reactions*  
8  
9

10 Next, we demonstrate the two above-mentioned principles by NMR kinetic  
11 measurements. We have studied stoichiometric C–H activation of 3-bromoacetanilide  
12  
13 (p*K*<sub>a</sub> ≈ -4.4) and *N,N*-dimethylbenzylamine (p*K*<sub>a</sub> ≈ 9); two substrates found on the  
14  
15 opposite ends of the acidity scale (for details see Experimental section S13). The kinetic  
16  
17 profiles of C–H activation of 3-bromoacetanilide are shown in Figures 4a,b. These  
18  
19 diagrams illustrate that the rate of C–H activation increases with the increasing acidity  
20  
21 strength from dichloroacetic acid to TFA. In the case of weaker chloroacetic or acetic  
22  
23 acids the palladium is so unreactive that the reaction does not occur at all. On the other  
24  
25 hand, the kinetic profiles of C–H activation of basic *N,N*-dimethylbenzylamine (Fig. 4c)  
26  
27 show different behavior. With increasing acidity of the additional acid, the conversion of  
28  
29 the substrate to the organopalladium complex decreases. The decreased conversion is  
30  
31 caused by the added acids that protonate the substrate and thus prevent its  
32  
33 coordination to the palladium complex. The protonation is visible in the NMR spectra as  
34  
35 the splitting of the signals of CH<sub>2</sub> and CH<sub>3</sub> groups of *N,N*-dimethylbenzylamine (Figure  
36  
37  
38  
39  
40  
41  
42  
43  
44  
45  
46  
47  
48  
49  
50  
51  
52  
53  
54  
55  
56  
57  
58  
59  
60

S22) analogous to the splitting in the titration experiments. Furthermore, the amount of unreacted substrate seems to be linearly dependent on PA of the added acids (Figure S24).

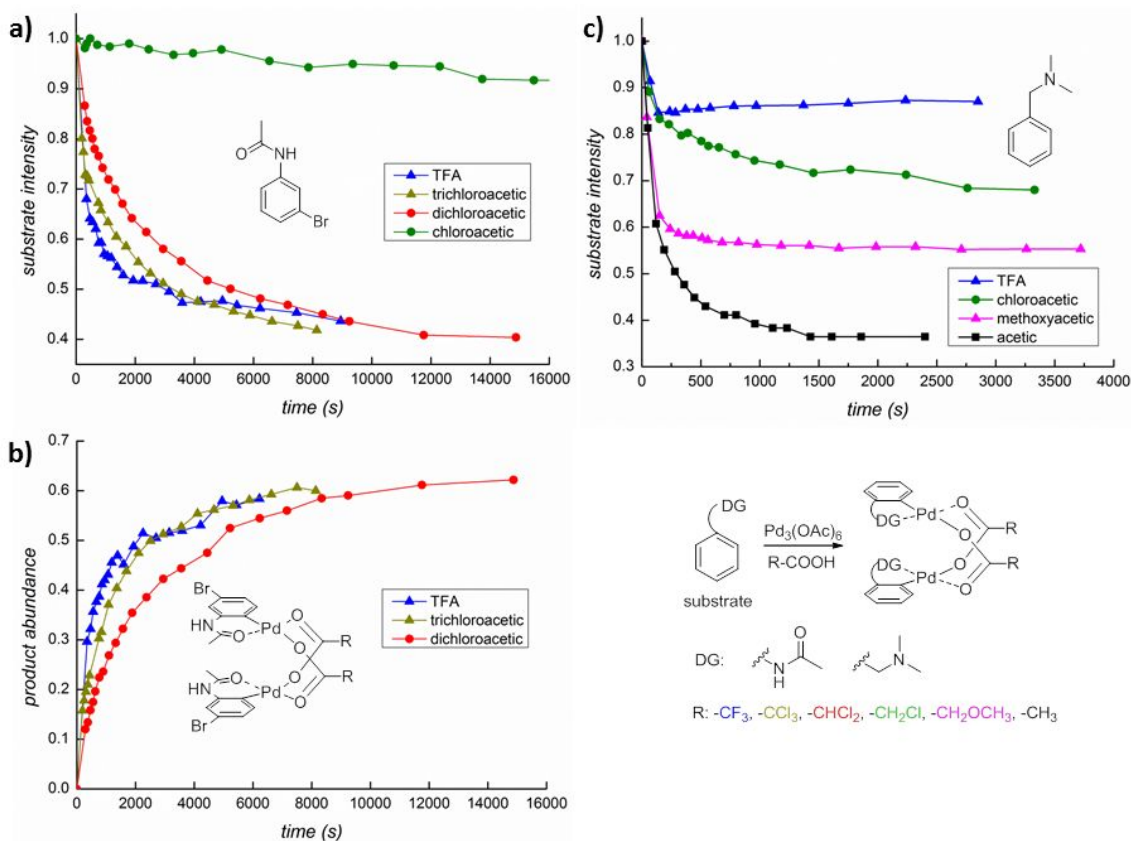


**Figure 4.** The  $^1\text{H}$  NMR kinetic profiles of C–H activation of 3-bromoacetanilide (a,b) and *N,N*-dimethylbenzylamine (c) in presence of palladium(II) acetate (0.66 equiv.) and additional acids (4.4 eq.) in DCM at 25 °C.

#### *Selection of the optimal added acid*

1  
2  
3 The obtained findings illustrate the opposing effects of the added acids. On one hand,  
4  
5  
6  
7 addition of strong acids leads to the formation of more active catalyst and thus to  
8  
9  
10 acceleration of the reaction. On the other hand, the acid can protonate the substrate  
11  
12  
13 which retards the reaction. In other words, optimal added acid should be as strong as  
14  
15  
16 possible, but it must not fully protonate the substrate. Finding a balance between these  
17  
18  
19 two principles leads to an easier design of optimal reaction conditions.  
20  
21  
22  
23

24 Good starting point for selecting the optimal additive is to compare acidities of the  
25  
26  
27 added acids with acidities of protonated form of the substrate. Obviously, these values  
28  
29  
30 should be as close as possible. Using organic solvents for C–H functionalization  
31  
32  
33 reactions offers larger selection of suitable acidity parameters. Apart from  $pK_a$  known in  
34  
35  
36 most cases only in water, these could be for instance  $PA^{11}$  or  $\Delta H_D^{0.13}$ . We believe that  
37  
38  
39 predicted  $pK_a$  values from available software like e.g., MarvinSketch<sup>19</sup> provide a  
40  
41  
42 sufficient estimate. However, other acidity parameters in solvent of interest can provide  
43  
44  
45 more accurate results. For an easier visualization, we will use a tentative diagram in Fig.  
46  
47  
48  
49  
50  
51  
52 5.  
53  
54  
55  
56  
57  
58  
59  
60

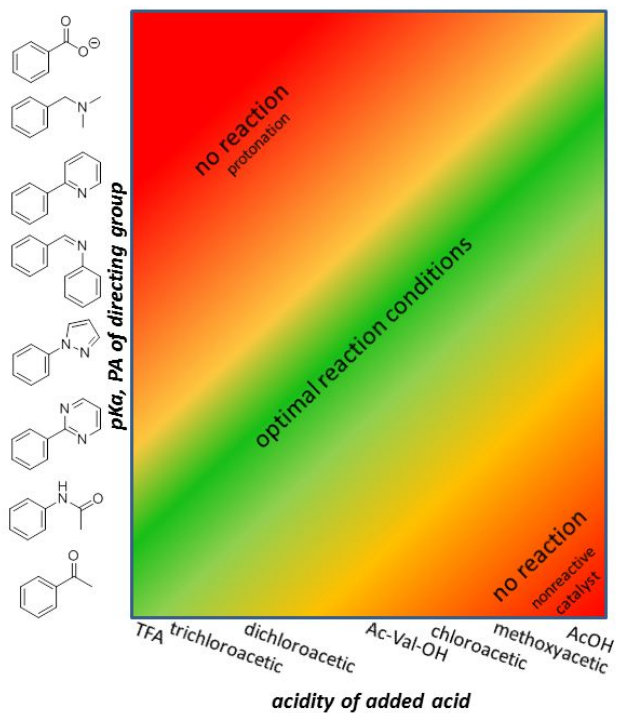


**Figure 5.** Diagram correlating acidity (in terms of  $pK_a$ , PA,  $\Delta H_D^0$ , etc.) of some typical substrates and added acids with reactivity. The diagram predicts suitable added acids for C–H activation of the substrates.

The diagram correlates acidity parameters for typical substrates with acidity of the added acids. Red areas correspond to the improper substrate/additive combination due to the protonation of the substrate (left upper corner) or not enough reactive catalyst (right bottom corner). The green area corresponds to the optimal substrate/additive combinations enabling reactions to run fast even at lower temperatures.

The idealized workflow for selection is as follows:

- 1) selection of substrate of interest;
- 2) selection of the solvent;
- 3) prediction or measurement of substrate  $pK_a$  (or other acidity parameter);
- 4) selection of appropriate additional acid;
- 5) final optimization of reaction conditions including other reaction components and temperature.

This workflow can be used under the assumption that the added acid cannot react with substrate, functionalizing reagents or product.

#### *Proof of concept experiments in catalytic arrangement*

To validate the concept, we determined yields of several C–H functionalization reactions in dependence of acidities of the added acids. We have chosen two substrates located on the opposite sides of the basicity scale (acetanilide and 2-phenylpyridine). To obtain consistent data with the previous mechanistic experiments, we tried to find reactions proceeding in DCM at room temperature. Even though these are not optimum conditions found in literature and the observed yields are thus reduced.

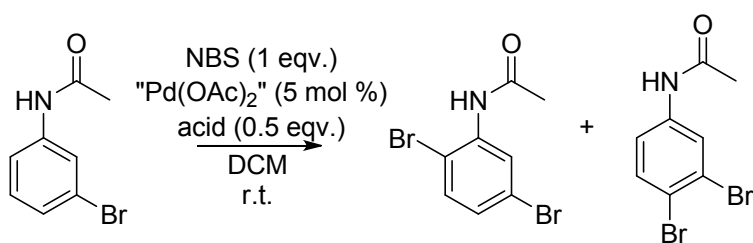
1  
2  
3 Furthermore, we summarized the effect of the added acids on the yields for some of the  
4  
5  
6  
7 typical substrates found in literature (S23-26). We are aware of the complex nature of  
8  
9  
10 the reaction mixtures and of the fact that the added acids may affect also other  
11  
12  
13 elementary reactions than just C–H activation and substrate protonation. Nevertheless,  
14  
15  
16 this is always the case and the selected examples give a hint how the basicity of the  
17  
18  
19 substrate affects the acid effect.  
20  
21  
22  
23  
24  
25

26 *Acetanilides* ( $pK_a \approx -4$ )  
27  
28

29 Literature retrieval shows (Table S7-9) that addition of stronger acids like TFA or *p*-  
30  
31  
32 toluenesulfonic acids to the reaction mixtures is either necessary or at least improves  
33  
34  
35 the yields.<sup>20</sup> Furthermore Brown et al. showed increasing reaction rate with increasing  
36  
37  
38 amount of added *p*-toluenesulfonic acid.<sup>21</sup>  
39  
40  
41  
42

43 According to Bedford<sup>22</sup> the 3-bromoacetanilide is brominated by NBS to give a mixture  
44  
45  
46 of *ortho* and *para* brominated products (Scheme 3). The *para* bromination proceeds *via*  
47  
48  
49 classical electrophilic aromatic substitution where electrophile is generated by the  
50  
51  
52 reaction of NBS with acid. Table 3 shows that chloroacetic and dichloroacetic acids give  
53  
54  
55  
56  
57  
58  
59  
60

the best yields. The *ortho* bromination product is formed predominantly by the palladium catalyzed directed C–H functionalization. Comparison of the yields in Table 3 shows the predicted decrease of the yields of *ortho* bromination with decreasing acidity strength. The same reactivity trend was observed in the case of oxidative acylation of acetanilides inspired by work of Novak and co-workers (Table S3).<sup>20a</sup>



**Scheme 3.** Bromination of 3-bromoacetanilide using NBS.

**Table 3.** Yields of bromination of 3-bromoacetanilide determined after 24 hours.

acid	yield <sup>a</sup> <i>ortho</i>	yield <sup>a</sup> <i>para</i>
TFA	33 (36) <sup>b</sup>	28 (27) <sup>b</sup>
trichloroacetic	30	32



dichloroacetic	16	41
chloroacetic	6	37
methoxyaceti	2	34
c		
Ac-Val-OH	0	29
AcOH	0	15

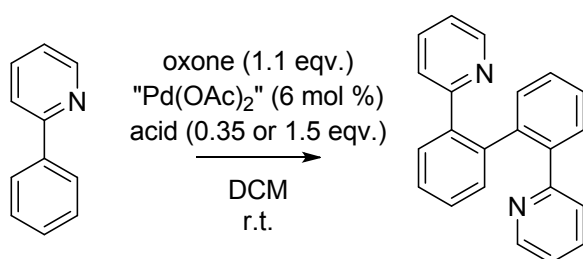
<sup>a</sup> determined by <sup>1</sup>H NMR of the crude mixture

<sup>b</sup> isolated yield from independent experiment after 24 hours

### *2-Phenylpyridines (pK<sub>a</sub> ≈ 4.4)*

Typical protocols<sup>23</sup> for functionalization of 2-phenylpyridines usually do not use acidic additives. However, some exceptions are known (Table S12).<sup>24</sup> To demonstrate the acidity effect, we followed dimerization of 2-phenylpyridine<sup>25</sup> (Ph-Py) (Scheme 4). The pK<sub>a</sub> value of protonated 2-phenylpyridine (4.4 in water) lies between the values of acetic

1  
2  
3  
4 (pK<sub>a</sub> ≈ 4.7) and methoxyacetic (pK<sub>a</sub> ≈ 3.4) acids. In the experiments, we used 0.35 and  
5  
6  
7 1.5 equivalents of acids to see the effects of protonation (Table 4). The results show  
8  
9  
10 that in the case of sub-stoichiometric amount of acid, the methoxyacetic acid is the best  
11  
12  
13  
14 additive. However, in the case of 1.5 equivalents of the additives, the weaker acetic acid  
15  
16  
17 is the most efficient one.  
18  
19  
20  
21  
22  
23  
24



34 **Scheme 4.** Dimerization of 2-phenylpyridine.  
35  
36  
37  
38  
39  
40  
41

42 **Table 4.** Yields<sup>a</sup> of dimerization of 2-phenylpyridine determined after 4 hours.  
43  
44  
45

Acid	0.35 equiv. acid <sup>c</sup>	1.5 equiv. acid <sup>c</sup>
TFA	9	21

46  
47  
48  
49  
50  
51  
52  
53  
54  
55  
56  
57  
58  
59  
60

1  
2  
3  
4  
5  
6  
7  
8  
9  
10  
11  
12  
13  
14  
15  
16  
17  
18  
19  
20  
21  
22  
23  
24  
25  
26  
27  
28  
29  
30  
31  
32  
33  
34  
35  
36  
37  
38  
39  
40  
41  
42  
43  
44  
45  
46  
47  
48  
49  
50  
51  
52  
53  
54  
55  
56  
57  
58  
59  
60

trichloroacetic	17	18
dichloroacetic	15	22
chloroacetic	16	23
methoxyaceti	<b>47</b>	20
<b>c</b>		
Ac-Val-OH	35	21
AcOH	21	<b>54 (50)<sup>b</sup></b>
without acid		17

<sup>a</sup> determined by <sup>1</sup>H NMR of the crude mixture.

<sup>b</sup> isolated yield from independent experiment after 5 hours

<sup>c</sup> acid equivalents are with respect to 2-phenylpyridine

Further, we followed time dependence of the palladium-catalyzed dimerization with addition of methoxyacetic and acetic acids in detail. In the case of acetic acid, the increasing amount of the acid (from 0 to 1.5 equivalents) correlates with the increasing

1  
2  
3 yield of the dimerization reaction (Figure S27). Further increase of the amount of acid  
4  
5  
6  
7 above 1.5 equiv. does not improve the yield.  
8  
9

10 In the case of methoxyacetic acid, the best yields were achieved with addition of 0.2–  
11  
12 0.4 equivalents of acid with respect to 2-phenylpyridine (Figure S28). The reaction  
13  
14 proceeds with 6 mol % of Pd(OAc)<sub>2</sub>. Hence, for the exchange of acetate ligands by  
15  
16 methoxyacetate, we need 0.12 equivalents of the added acid. The results thus suggest  
17  
18 that we achieve the best conversion under the conditions that allow ligand exchange,  
19  
20 but do not provide a large excess of the free acid in solution. This is in agreement with  
21  
22 the presumption that the increasing acidity of the acid facilitates the reaction but  
23  
24 reduces amount of available substrate by its protonation. Figure 6 illustrate these  
25  
26 observations. At the beginning of the reaction (Figure 6 on the top) the reaction is faster  
27  
28 in presence of small amount of methoxyacetic acid. The increasing amount of  
29  
30 methoxyacetic acid reduces the yields and acetic acid becomes more efficient additive  
31  
32 under such conditions. At long reaction times, acetic acid is the better additive even at  
33  
34 the lower concentrations. Finally, in the presence of strong acids, the reaction takes  
35  
36 place faster, but with less efficiency.  
37  
38  
39  
40  
41  
42  
43  
44  
45  
46  
47  
48  
49  
50  
51  
52  
53  
54  
55  
56  
57  
58  
59  
60

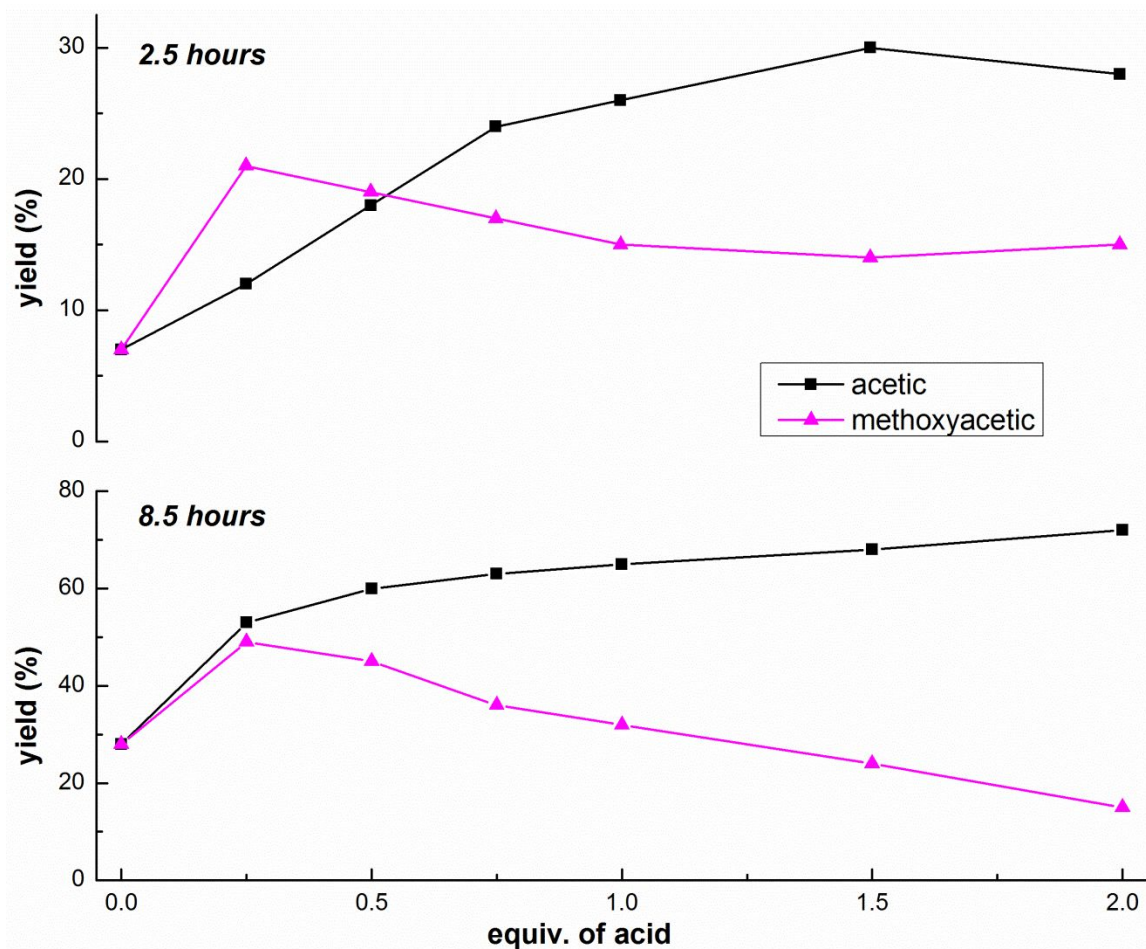


**Figure 6.** Dependence of yields of dimerization of 2-phenylpyridine determined after 2.5 (top) and 8.5 (bottom) hours on amount of added acetic (black) or methoxyacetic (purple) acids.

The answer to the question “What is the optimal amount of the added acid?” is not straightforward. This depends on the factors such as difference between  $pK_a$ s of the substrate and expected product or  $pK_a$ s of the other reaction components. These species can bind the acid more strongly than the substrate and leave it free for the

1  
2  
3 reaction. Furthermore, the whole reaction system is in equilibrium. Thus non-protonated  
4  
5  
6  
7 substrate can be present in the reaction mixture in a small amount even in the presence  
8  
9  
10 of strong acids allowing its C–H activation by the reactive catalyst, especially at elevated  
11  
12  
13  
14 temperatures.

15  
16  
17 Recently, mono-*N*-protected amino acids (MPAA) were found to be very efficient  
18  
19  
20 additives in this type of reactions.<sup>26</sup> Their role in reaction mechanisms is still a highly  
21  
22  
23 discussed topic.<sup>27</sup> Therefore, we included *N*-acetylvaline (Ac-Val-OH) ( $pK_a \approx 3.7$ )<sup>14</sup> into  
24  
25  
26  
27 the experiments in order to test, whether part the positive effect of MPAA can originate  
28  
29  
30  
31 by their increased  $pK_a$  values in comparison to acetic acid. The observed yields in  
32  
33  
34  
35 Tables 3,4 suggest that Ac-Val-OH fits into the scale of acids. Thus, its increased ability  
36  
37  
38 to activate palladium should be involved in the discussions of the mechanism of action  
39  
40  
41  
42 of MPAA.

## 43 44 45 46 47 48 49 CONCLUSIONS

50  
51  
52 This work offers a simple workflow that allows for an easier selection of additional  
53  
54  
55  
56 carboxylic acids in palladium carboxylates catalyzed C–H functionalization reactions  
57  
58  
59  
60

1  
2  
3 assisted by directing groups. The scheme is based on two opposing effects of additional  
4  
5  
6  
7 acids; protonation of the substrate and formation of a more active catalyst. The most  
8  
9  
10 appropriate additive should have acidity close to the acidity of conjugated acid of the  
11  
12  
13 substrate. The comparison of predicted  $pK_a$  values has been shown to be sufficient for  
14  
15  
16 this approach. Due to the complexity of reaction systems, it is difficult to exactly predict  
17  
18  
19 the nature and optimal amount of added acid. However, we illustrated that usage of less  
20  
21  
22 common additional acids can help to run reactions with better yields and at lower  
23  
24  
25 temperatures. In other words, it helps to improve reaction economy. Furthermore, the  
26  
27  
28 positive effect of mono-*N*-protected amino acids is discussed in the context of increased  
29  
30  
31 electrophilicity of palladium connected to these ligands. Last but not least, this approach  
32  
33  
34 opens up the possibility of protonation driven regioselectivity tuning in substrates  
35  
36  
37  
38  
39  
40  
41 containing more directing groups.  
42  
43  
44  
45  
46  
47  
48  
49

## 50 EXPERIMENTAL AND COMPUTATIONAL DETAILS

### 51 52 53 54 55 **Materials and methods** 56 57 58 59 60

1  
2  
3 All the chemicals and solvents were purchased from Acros Organics, Sigma-Aldrich or  
4  
5  
6  
7 Fluorochem and used as received. High resolution mass spectra were recorded on a  
8  
9  
10 MALDI LTQ Orbitrap XL equipped with nitrogen UV laser (337 nm, 60 Hz, 8-20  $\mu$ J) in  
11  
12  
13  
14 positive ion mode. The NMR spectra were recorded on a Bruker Avance III 400 MHz or  
15  
16  
17 on a Bruker Ascend 500 MHz instruments. Chemical shifts  $\delta$  are referenced to TMS ( $\delta$  =  
18  
19  
20 0 ppm) or solvent residual peaks  $\delta(\text{CD}_2\text{Cl}_2) = 5.35$  ppm ( $^1\text{H}$ ),  $\delta(\text{DMSO-d}_6) = 2.55$  ppm  
21  
22  
23  
24 ( $^1\text{H}$ ).  
25  
26  
27  
28

29 **Ligand exchange experiments** In a typical experiment, 10 mg (0.0445 mmol) of  
30  
31  
32 palladium(II) acetate was dissolved in 0.7 ml of  $\text{CD}_2\text{Cl}_2$  in NMR tube and 2  $\mu\text{L}$   
33  
34  
35 trifluoromethylbenzene were added as a standard. The five molar excess (0.223 mmol)  
36  
37  
38 of carboxylic acid was added and the  $^1\text{H}$  NMR kinetics was followed. The rate constants  
39  
40  
41  
42 were obtained from the first-order fits of decrease of signals of acetate ligands  
43  
44  
45  
46 coordinated to palladium.  
47  
48  
49

50  
51 **Titration experiments** In a typical experiment, the carboxylic acids were added in small  
52  
53  
54 increments to the solution of 50  $\mu\text{L}$  (0.335 mmol) of DMBA (or other substrates)  
55  
56  
57  
58  
59  
60



1  
2  
3 dissolved in 0.5 ml of CD<sub>2</sub>Cl<sub>2</sub> in NMR tube. The <sup>1</sup>H NMR spectra were recorded after  
4  
5  
6  
7 each addition. Chloroacetic and trichloroacetic acids were added in melted form.  
8  
9

10  
11 **Kinetics of C–H activation reactions** In a typical experiment, the carboxylic acid (0.3  
12  
13 mmol) was added to the solution of 10 mg (0.045 mmol) of palladium(II)acetate  
14  
15 dissolved in 0.4 ml of CD<sub>2</sub>Cl<sub>2</sub> (in the case of DMBA containing 5 μL of CH<sub>2</sub>Br<sub>2</sub> as a  
16  
17  
18 standard) in NMR tube. After 10 minutes the solution of substrate (0.068 mmol)  
19  
20  
21 dissolved in 0.1 ml CD<sub>2</sub>Cl<sub>2</sub> was added and the <sup>1</sup>H NMR spectra were recorded in  
22  
23  
24  
25 increasing time intervals.  
26  
27  
28  
29  
30  
31

32  
33 **DFT calculations** All calculations were performed using the B3LYP density functional  
34  
35  
36 theory method as implemented in Gaussian09<sup>28</sup> with the D3 dispersion term using the  
37  
38  
39 Becke-Johnson damping function.<sup>29</sup> The basis set was a combination of the SDD  
40  
41  
42 pseudopotential model for palladium<sup>30</sup> and 6-311++G\*\* for all other atoms. The final  
43  
44  
45  
46 energies include solvation free energies in CH<sub>2</sub>Cl<sub>2</sub> determined by single-point  
47  
48  
49  
50 calculation for the optimized structures using the SMD model.<sup>31</sup>  
51  
52  
53  
54

55 **Characterization of the compounds**  
56  
57  
58  
59  
60

1  
2  
3  
4 *2,2'-di(pyridin-2-yl)-1,1'-biphenyl*. 2-phenylpyridine (0.275 mmol, 41  $\mu$ L) was added to the 4 ml vial  
5  
6 containing Oxone (0.31 mmol, 195 mg), palladium (II)acetate (0.0175 mmol, 3.9 mg), 2 ml of DCM and  
7  
8 0.41 mmol of acetic acid. The reaction was stirred under air at room temperature for 5 hours. The crude  
9  
10 reaction mixture was purified by silica gel column chromatography (ethyl-acetate/hexane). Isolated yield:  
11  
12 21 mg (50 %) of white solid.  $^1\text{H}$  NMR (500 MHz,  $\text{CDCl}_3$ ):  $\delta$  8.33 (d,  $^3J$  4.8 Hz, 2H); 7.55-7.51 (m, 2H);  
13  
14 7.46-7.38 (m, 6H); 7.33 (dt,  $^3J$  7.8 and 1.7 Hz, 2H); 7.02 (m, 2H).  $^{13}\text{C}\{^1\text{H}\}$  NMR (125 MHz,  $\text{CDCl}_3$ ):  $\delta$   
15  
16 157.9; 148.9; 139.9; 139.8; 135.3; 131.3; 130.0; 128.6; 127.8; 124.5; 121.2. HRMS (MALDI-orbitrap)  
17  
18 m/z:  $[\text{M} + \text{H}]^+$  Calcd for  $\text{C}_{22}\text{H}_{17}\text{N}_2$  309.13863; Found: 309.13854.

19 *2,5-dibromoacetanilide*. 3-Bromoacetanilide (0.25 mmol, 53.5 mg), NBS (0.251 mmol, 47 mg),  
20  
21 palladium (II)acetate (0.0125 mmol, 2.8 mg) and 1 ml of DCM were added to the 4 ml reaction vial,  
22  
23 followed by addition of 0.125 mmol of trifluoroacetic acid. The reaction was stirred at room temperature  
24  
25 for 24 hours and quenched with 2ml of brine/EtOAc (1:1) solution. Organic layer was evaporated and  
26  
27 purified by silica gel column chromatography (ethyl-acetate/hexane). Isolated yield: 26 mg (36 %) of  
28  
29 white solid.  $^1\text{H}$  NMR (500 MHz,  $\text{CDCl}_3$ ):  $\delta$  8.59 (s, 1H); 7.58 (bs, 1H); 7.39 (d,  $^3J$  8.55 Hz, 1H); 7.11  
30  
31 (dd,  $^3J$  8.55 and 2.29 Hz, 1H); 2.25 (s, 3H).  $^{13}\text{C}\{^1\text{H}\}$  NMR (125 MHz,  $\text{CDCl}_3$ ):  $\delta$  168.2; 136.7; 133.1;  
32  
33 128.0; 124.4; 122.1; 111.4; 25.0. HRMS (MALDI-orbitrap) m/z:  $[\text{M} + \text{H}]^+$  Calcd for  $\text{C}_8\text{H}_8\text{Br}_2\text{NO}$   
34  
35 291.89672; Found: 291.89704.

36 *N-(2-(4-chlorobenzoyl)phenyl)acetamide* Acetanilide (0.25 mmol, 33.7 mg), 4-chlorobenzaldehyde (0.5  
37  
38 mmol, 707 mg), palladium (II)acetate (0.0125 mmol, 2.8 mg) and 0.7 ml of DCM were added to the 4 ml  
39  
40 reaction vial, followed by addition of 0.125 mmol of trifluoroacetic acid and 100  $\mu$ L (2.1 eqv.) of TBHP  
41  
42 (5.5 M solution in decane). The reaction was stirred for 24 hours at room temperature. The crude reaction  
43  
44 mixture was purified by silica gel column chromatography (ethyl-acetate/hexane). Isolated yield: 16 mg  
45  
46 (23 %) of white solid  $^1\text{H}$  NMR (500 MHz,  $\text{CDCl}_3$ ):  $\delta$  10.71 (s, 1H); 8.61 (d,  $^3J$  8.38 Hz, 1H); 7.65 (d,  $^3J$   
47  
48 8.53 Hz, 2H); 7.59 (t,  $^3J$  7.42 Hz, 1H); 7.51 (d,  $^3J$  7.79 Hz, 1H); 7.47 (d,  $^3J$  8.50 Hz, 2H); 7.10 (t,  $^3J$   
49  
50 7.75 Hz, 1H); 2.23 (s, 3H).  $^{13}\text{C}\{^1\text{H}\}$  NMR (125 MHz,  $\text{CDCl}_3$ ):  $\delta$  198.4; 169.3; 140.4; 139.1; 136.8;  
51  
52 134.5; 133.2; 131.4; 128.7; 123.0; 122.2; 121.7; 25.3.  
53  
54  
55  
56  
57  
58  
59  
60

1  
2  
3  
4 ASSOCIATED CONTENT  
5  
6  
7

8 **Supporting Information.** Ligand exchange experiments, titration experiments, C–H  
9  
10  
11 activation experiments, proof of concept experiments, spectra and DFT calculation  
12  
13  
14  
15 results together with geometries of all optimized structures.  
16  
17  
18

19 The following files are available free of charge.  
20  
21  
22

23 Experimental details (PDF)  
24  
25

26 Optimized geometries (xyz)  
27  
28  
29  
30

31 AUTHOR INFORMATION  
32  
33  
34

35 **Corresponding Author**  
36  
37

38 \*jiri.vana@upce.cz  
39  
40  
41  
42

43 **Author Contributions**  
44  
45  
46

47 The manuscript was written through contributions of all authors. All authors have given  
48  
49  
50 approval to the final version of the manuscript.  
51  
52  
53

54 **Funding Sources**  
55  
56  
57  
58  
59  
60

GAČR 17-08499S.

## ACKNOWLEDGMENT

The authors acknowledge the financial support from the project GAČR 17-08499S.

## REFERENCES

- (1) Kapdi, A.; Maiti, D. Strategies for Palladium-Catalyzed Non-directed and Directed C- H Bond Functionalization, Elsevier **2017**, Paperback ISBN: 9780128052549.
- (2) (a) Chen, Z.; Wang, B.; Zhang, J.; Yu, W.; Liu, Z.; Zhang, Y. Transition metal-catalyzed C–H bond functionalizations by the use of diverse directing groups. *Org. Chem. Front.* **2015**, *2*, 1107–1295. (b) Sambigiato, C.; Schönbauer, D.; Blicek, R.; Dao-Huy, T.; Pototschnig, G.; Schaaf, P.; Wiesinger, T.; Zia, M. F.; Wencel-Delord, J.; Besset, T.; Maes, B. U. W.; Schnürch, M. A comprehensive overview of directing groups applied in metal-catalysed C–H functionalisation chemistry. *Chem. Soc. Rev.* **2018**, *47*, 6603-6743.

1  
2  
3  
4 (3) Engle, K. M.; Mei, T-S.; Wasa, M.; Yu, J.-Q. Weak Coordination as a Powerful  
5  
6  
7 Means for Developing Broadly Useful C-H Functionalization Reactions. *Acc. Chem.*  
8  
9  
10 *Res.* **2012**, *45*, 788-802.

11  
12  
13  
14 (4) Váňa, J.; Hanusek, J.; Sedlák, M. Bi and trinuclear complexes in palladium  
15  
16  
17 carboxylate-assisted C-H activation reactions. *Dalton Trans.* **2018**, *47*, 1378-1382.

18  
19  
20  
21  
22 (5) Desai, L. V.; Stowers, K. J.; Sanford, M. S. Insights into Directing Group Ability in  
23  
24  
25 Palladium-Catalyzed C-H Bond Functionalization. *J. Am. Chem. Soc.* **2008**, *130*,  
26  
27  
28  
29 13285–13293.

30  
31  
32  
33 (6) (a) Cai, G.; Fu, Y.; Li, Y.; Wan, X.; Shi, Z. Indirect *ortho* Functionalization of  
34  
35  
36 Substituted Toluenes through *ortho* Olefination of *N,N*-Dimethylbenzylamines Tuned by  
37  
38  
39 the Acidity of Reaction Conditions. *J. Am. Chem. Soc.* **2007**, *129*, 7666-7673. (b)  
40  
41  
42  
43 Roiban, G.-D.; Serrano, E.; Soler, T.; Aullón, G.; Grosu, I.; Cativiela, C.; Martínez, M.;  
44  
45  
46  
47 Urriolabeitia, E. P. Regioselective Orthopalladation of (Z)-2-Aryl-4-Arylidene-5(4H)-  
48  
49  
50 Oxazolones: Scope, Kinetic-Mechanistic, and Density Functional Theory Studies of the  
51  
52  
53  
54 C-H Bond Activation. *Inorg. Chem.* **2011**, *50*, 8132–8143. (c) Granell, J.; Martínez, M.  
55  
56  
57  
58  
59  
60

1  
2  
3  
4 Kinetico-mechanistic studies of cyclometalating C–H bond activation reactions on Pd(II)  
5  
6  
7 and Rh(II) centres: The importance of non-innocent acidic solvents in the process.  
8

9  
10 *Dalton Trans.* **2012**, *41*, 11243-11258. (d) Sanhueza, I. A.; Wagner, A. M.; Sanford, M.

11  
12  
13  
14 S.; Schoenebeck, F. On the role of anionic ligands in the site-selectivity of oxidative C–

15  
16  
17 H functionalization reactions of arenes. *Chem. Sci.*, **2013**, *4*, 2767-2775.  
18

19  
20  
21 (7) (a) Gray, A.; Tsybizova, A.; Roithová, J. Carboxylate-assisted C–H activation of  
22  
23  
24  
25 phenylpyridines with copper, palladium and ruthenium: a mass spectrometry and DFT  
26  
27  
28 study. *Chem. Sci.* **2015**, *6*, 5544–5553. (b) Lebrasseur, N.; Larrosa, I. Room

29  
30  
31  
32 Temperature and Phosphine Free Palladium Catalyzed Direct C-2 Arylation of Indoles.  
33

34  
35  
36 *J. Am. Chem. Soc.* **2008**, *130*, 2926-2927.  
37

38  
39  
40 (8) Davies, D. L.; Macgregor, S. A.; McMullin, C. L. Computational Studies of  
41  
42  
43 Carboxylate-Assisted C–H Activation and Functionalization at Group 8–10 Transition  
44  
45  
46  
47 Metal Centers. *Chem. Rev.* **2017**, *117*, 8649-8709.  
48

49  
50  
51 (9) Dudkina, Y. B.; Kholin, K. V.; Gryaznova, T. V.; Islamov, D. R.; Kataeva, O. N.;  
52  
53  
54  
55 Rizvanov, I. Kh.; Levitskaya, A. I.; Fominykh, O. D.; Balakina, M. Yu.; Sinyashina, O. G.;  
56  
57  
58

1  
2  
3 Budnikova, Y. H. Redox trends in cyclometalated palladium(II) Complexes. *Dalton*  
4  
5  
6  
7 *Trans.* **2017**, *46*, 165-177.  
8  
9

10  
11 (10) Váňa, J.; Lang, J.; Šoltésová, M.; Hanusek, J.; Růžička, A. Sedlák, M.; Roithová,  
12  
13  
14 J. The role of trinuclear species in a palladium acetate/trifluoroacetic acid catalytic  
15  
16  
17  
18 system. *Dalton Trans.* **2017**, *46*, 16269–16275.  
19  
20

21  
22 (11) The pKa values are taken from: <https://www.chem.wisc.edu/areas/organic/index->  
23  
24  
25  
26 chem.htm, The PA values are taken from: Pérez, P.; Toro-Labbé, A. Global and Local  
27  
28  
29 Analysis of the Gas-Phase Acidity of Haloacetic Acids. *J. Phys. Chem. A* **2000**, *104*,  
30  
31  
32  
33 5882-5887.  
34  
35

36  
37 (12) values related to the acetic acid  
38  
39

40  
41 (13) Cumming, J. B.; Kebarle, P. Summary of gas phase acidity measurements  
42  
43  
44  
45 involving acids AH. Entropy changes in proton transfer reactions involving negative  
46  
47  
48 ions. Bond dissociation energies  $D(A-H)$  and electron affinities  $EA(A)$ . *Can. J. Chem.*  
49  
50  
51  
52 **1978**, *56*, 1-9.  
53  
54  
55  
56  
57  
58  
59  
60

1  
2  
3  
4 (14) King, E. J.; King, G. W. The Thermodynamics of Ionization of Amino Acids. II.  
5  
6  
7 The Ionization Constants of Some N-Acyl Amino Acids. *J. Am. Chem. Soc.* **1956**, *78*,  
8  
9  
10 1089–1099.

11  
12  
13  
14 (15) (a) <http://supramolecular.org/> (b) Thordarson, P. Determining association  
15  
16  
17 constants from titration experiments in supramolecular chemistry. *Chem. Soc.*  
18  
19  
20  
21 *Rev.*, **2011**, *40*, 1305-1323. (c) Hibbert, D. B.; Thordarson, P. The death of the Job plot,  
22  
23  
24  
25 transparency, open science and online tools, uncertainty estimation methods and other  
26  
27  
28  
29 developments in supramolecular chemistry data analysis. *Chem. Commun.* **2016**, *52*,  
30  
31  
32 12792-12805.

33  
34  
35  
36 (16) (a) Váňa, J.; Petrović, V.; Terencio, T.; Tischler, O.; Novák, Z.; Roithová, J.  
37  
38  
39  
40 Palladium-Catalyzed C–H Activation: Mass Spectrometric Approach to Reaction  
41  
42  
43 Kinetics in Solution. *Organometallics* **2017**, *36*, 2072. (b) Tischler, O.; Kovács, S.;  
44  
45  
46  
47 Érseka, G.; Králl, P.; Darub, J.; Stirling, A.; Novák, Z. Study of Lewis acid accelerated  
48  
49  
50  
51 palladium catalyzed C–H activation. *J. Mol. Catal. A-Chem.* **2017**, *426*, 444–45.



1  
2  
3  
4 (17) Jia, C.; Piao, D.; Oyamada, J.; Lu, W.; Kitamura T.; Fujiwara, Y. Efficient  
5  
6  
7 activation of aromatic C-H bonds for addition to C-C multiple bonds. *Science* **2000**, *287*,  
8  
9  
10 1992-1995.

11  
12  
13  
14 (18) (a) We have based our calculations of the *N,N*-dimethylbenzylamine system on  
15  
16  
17  
18 Macgregor geometries: Davies, D. L.; Donald, S. M. A.; Macgregor, S. A. Computational  
19  
20  
21  
22 Study of the Mechanism of Cyclometalation by Palladium Acetate. *J. Am. Chem. Soc.*  
23  
24  
25 **2005**, *127*, 13754-13755. (b) Sajjad, M. A.; Harrison, J. A.; Nielson, A. J. NBO Orbital  
26  
27  
28  
29 Interaction Analysis for the Ambiphilic Metal-Ligand Activation/Concerted Metalation  
30  
31  
32  
33 Deprotonation (AMLA/CMD) Mechanism Involved in the Cyclopalladation Reaction of  
34  
35  
36 *N,N*-Dimethylbenzylamine with Palladium Acetate. *Organometallics* **2018**, *37*,  
37  
38  
39 3659-3669.

40  
41  
42  
43 (19) <https://chemaxon.com/products/marvin>

44  
45  
46  
47 (20) (a) Szabó, F.; Daru, J.; Simkó, D.; Nagy, T. Z.; Stirling, A.; Novák, Z. Mild  
48  
49  
50  
51 Palladium-Catalyzed Oxidative Direct *ortho*-C-H Acylation of Anilides under Aqueous  
52  
53  
54  
55 Conditions. *Adv. Synth. Catal.* **2013**, *355*, 685-691. (b) Yang, F.; Song, F.; Li, W.; Lana,  
56  
57  
58  
59

1  
2  
3 J.; You, J. Palladium-catalyzed C–H activation of anilides at room temperature: *ortho*-  
4  
5  
6  
7 arylation and acetoxylation. *RSC Adv.* **2013**, *3*, 9649-9652. (c) Kim, B. S.; Dong, C. J.;  
8  
9  
10 Lee, J.; Youn, S. W. Highly Effective Pd-Catalyzed *ortho* Olefination of Acetanilides:  
11  
12  
13  
14 Broad Substrate Scope and High Tolerability. *Chem. Asian. J.* **2010**, *5*, 2336-2340.  
15  
16  
17

18 (21) Rauf, W.; Thompson, A. L.; Brown, J. M. Anilide activation of adjacent C–H bonds  
19  
20  
21 in the palladium-catalysed Fujiwara–Moritani reaction. *Dalton Trans.* **2010**, *39*, 10414-  
22  
23  
24  
25 10421.  
26  
27  
28

29 (22) Bedford, R. B.; Haddow, M. F.; Mitchell, C. J.; Webster, R. L. Mild C-H  
30  
31  
32 halogenation of anilides and the isolation of an unusual palladium(I)-palladium(II)  
33  
34  
35  
36 species. *Angew. Chem. Int. Ed.* **2011**, *50*, 5524-5527.  
37  
38  
39

40 (23) Kalyani, D.; Deprez, N. R.; Desai, L. V.; Sanford, M. S. Oxidative C–H  
41  
42  
43  
44 Activation/C–C Bond Forming Reactions: Synthetic Scope and Mechanistic Insights. *J.*  
45  
46  
47  
48 *Am. Chem. Soc.* **2005**, *127*, 7330–7331.  
49  
50  
51  
52  
53  
54  
55  
56  
57  
58  
59  
60

1  
2  
3  
4 (24) Yu, W.-Y.; Sit, W. N.; Zhou, Z.; Chan, A. S.-C. Palladium-Catalyzed  
5  
6  
7 Decarboxylative Arylation of C–H Bonds by Aryl Acylperoxides. *Org. Lett.* **2009**, *11*,  
8  
9  
10 3174-3177.

11  
12  
13  
14 (25) Hull, K. L.; Lanni, E. L.; Sanford, M. S. Highly Regioselective Catalytic Oxidative  
15  
16  
17  
18 Coupling Reactions: Synthetic and Mechanistic Investigations. *J. Am. Chem. Soc.*  
19  
20  
21  
22 **2006**, *128*, 14047–14049.

23  
24  
25  
26 (26) Engle, K. M.; Wang, D.-H.; Yu, J.-Q. Ligand-Accelerated C–H Activation  
27  
28  
29  
30 Reactions: Evidence for a Switch of Mechanism *J. Am. Chem. Soc.* **2010**, *132*, 14137–  
31  
32  
33 14151.

34  
35  
36  
37 (27) (a) Haines, B. E.; Yu, J.-Q.; Musaev, D. G. Enantioselectivity Model for Pd-  
38  
39  
40  
41 Catalyzed C–H Functionalization Mediated by the Mono-N-protected Amino Acid  
42  
43  
44 (MPAA) Family of Ligands. *ACS Catal.* **2017**, *7*, 4344–4354. (b) Musaev, D. G.; Kaledin,  
45  
46  
47  
48 A.; Shi, B.-F.; Yu, J.-Q. Key Mechanistic Features of Enantioselective C–H Bond  
49  
50  
51  
52 Activation Reactions Catalyzed by [(Chiral Mono-N-Protected Amino Acid)–Pd(II)]  
53  
54  
55  
56  
57  
58  
59  
60  
61  
62  
63  
64  
65  
66  
67  
68  
69  
70  
71  
72  
73  
74  
75  
76  
77  
78  
79  
80  
81  
82  
83  
84  
85  
86  
87  
88  
89  
90  
91  
92  
93  
94  
95  
96  
97  
98  
99  
100  
101  
102  
103  
104  
105  
106  
107  
108  
109  
110  
111  
112  
113  
114  
115  
116  
117  
118  
119  
120  
121  
122  
123  
124  
125  
126  
127  
128  
129  
130  
131  
132  
133  
134  
135  
136  
137  
138  
139  
140  
141  
142  
143  
144  
145  
146  
147  
148  
149  
150  
151  
152  
153  
154  
155  
156  
157  
158  
159  
160  
161  
162  
163  
164  
165  
166  
167  
168  
169  
170  
171  
172  
173  
174  
175  
176  
177  
178  
179  
180  
181  
182  
183  
184  
185  
186  
187  
188  
189  
190  
191  
192  
193  
194  
195  
196  
197  
198  
199  
200  
201  
202  
203  
204  
205  
206  
207  
208  
209  
210  
211  
212  
213  
214  
215  
216  
217  
218  
219  
220  
221  
222  
223  
224  
225  
226  
227  
228  
229  
230  
231  
232  
233  
234  
235  
236  
237  
238  
239  
240  
241  
242  
243  
244  
245  
246  
247  
248  
249  
250  
251  
252  
253  
254  
255  
256  
257  
258  
259  
260  
261  
262  
263  
264  
265  
266  
267  
268  
269  
270  
271  
272  
273  
274  
275  
276  
277  
278  
279  
280  
281  
282  
283  
284  
285  
286  
287  
288  
289  
290  
291  
292  
293  
294  
295  
296  
297  
298  
299  
300  
301  
302  
303  
304  
305  
306  
307  
308  
309  
310  
311  
312  
313  
314  
315  
316  
317  
318  
319  
320  
321  
322  
323  
324  
325  
326  
327  
328  
329  
330  
331  
332  
333  
334  
335  
336  
337  
338  
339  
340  
341  
342  
343  
344  
345  
346  
347  
348  
349  
350  
351  
352  
353  
354  
355  
356  
357  
358  
359  
360  
361  
362  
363  
364  
365  
366  
367  
368  
369  
370  
371  
372  
373  
374  
375  
376  
377  
378  
379  
380  
381  
382  
383  
384  
385  
386  
387  
388  
389  
390  
391  
392  
393  
394  
395  
396  
397  
398  
399  
400  
401  
402  
403  
404  
405  
406  
407  
408  
409  
410  
411  
412  
413  
414  
415  
416  
417  
418  
419  
420  
421  
422  
423  
424  
425  
426  
427  
428  
429  
430  
431  
432  
433  
434  
435  
436  
437  
438  
439  
440  
441  
442  
443  
444  
445  
446  
447  
448  
449  
450  
451  
452  
453  
454  
455  
456  
457  
458  
459  
460  
461  
462  
463  
464  
465  
466  
467  
468  
469  
470  
471  
472  
473  
474  
475  
476  
477  
478  
479  
480  
481  
482  
483  
484  
485  
486  
487  
488  
489  
490  
491  
492  
493  
494  
495  
496  
497  
498  
499  
500  
501  
502  
503  
504  
505  
506  
507  
508  
509  
510  
511  
512  
513  
514  
515  
516  
517  
518  
519  
520  
521  
522  
523  
524  
525  
526  
527  
528  
529  
530  
531  
532  
533  
534  
535  
536  
537  
538  
539  
540  
541  
542  
543  
544  
545  
546  
547  
548  
549  
550  
551  
552  
553  
554  
555  
556  
557  
558  
559  
560  
561  
562  
563  
564  
565  
566  
567  
568  
569  
570  
571  
572  
573  
574  
575  
576  
577  
578  
579  
580  
581  
582  
583  
584  
585  
586  
587  
588  
589  
590  
591  
592  
593  
594  
595  
596  
597  
598  
599  
600  
601  
602  
603  
604  
605  
606  
607  
608  
609  
610  
611  
612  
613  
614  
615  
616  
617  
618  
619  
620  
621  
622  
623  
624  
625  
626  
627  
628  
629  
630  
631  
632  
633  
634  
635  
636  
637  
638  
639  
640  
641  
642  
643  
644  
645  
646  
647  
648  
649  
650  
651  
652  
653  
654  
655  
656  
657  
658  
659  
660  
661  
662  
663  
664  
665  
666  
667  
668  
669  
670  
671  
672  
673  
674  
675  
676  
677  
678  
679  
680  
681  
682  
683  
684  
685  
686  
687  
688  
689  
690  
691  
692  
693  
694  
695  
696  
697  
698  
699  
700  
701  
702  
703  
704  
705  
706  
707  
708  
709  
710  
711  
712  
713  
714  
715  
716  
717  
718  
719  
720  
721  
722  
723  
724  
725  
726  
727  
728  
729  
730  
731  
732  
733  
734  
735  
736  
737  
738  
739  
740  
741  
742  
743  
744  
745  
746  
747  
748  
749  
750  
751  
752  
753  
754  
755  
756  
757  
758  
759  
760  
761  
762  
763  
764  
765  
766  
767  
768  
769  
770  
771  
772  
773  
774  
775  
776  
777  
778  
779  
780  
781  
782  
783  
784  
785  
786  
787  
788  
789  
790  
791  
792  
793  
794  
795  
796  
797  
798  
799  
800  
801  
802  
803  
804  
805  
806  
807  
808  
809  
810  
811  
812  
813  
814  
815  
816  
817  
818  
819  
820  
821  
822  
823  
824  
825  
826  
827  
828  
829  
830  
831  
832  
833  
834  
835  
836  
837  
838  
839  
840  
841  
842  
843  
844  
845  
846  
847  
848  
849  
850  
851  
852  
853  
854  
855  
856  
857  
858  
859  
860  
861  
862  
863  
864  
865  
866  
867  
868  
869  
870  
871  
872  
873  
874  
875  
876  
877  
878  
879  
880  
881  
882  
883  
884  
885  
886  
887  
888  
889  
890  
891  
892  
893  
894  
895  
896  
897  
898  
899  
900  
901  
902  
903  
904  
905  
906  
907  
908  
909  
910  
911  
912  
913  
914  
915  
916  
917  
918  
919  
920  
921  
922  
923  
924  
925  
926  
927  
928  
929  
930  
931  
932  
933  
934  
935  
936  
937  
938  
939  
940  
941  
942  
943  
944  
945  
946  
947  
948  
949  
950  
951  
952  
953  
954  
955  
956  
957  
958  
959  
960  
961  
962  
963  
964  
965  
966  
967  
968  
969  
970  
971  
972  
973  
974  
975  
976  
977  
978  
979  
980  
981  
982  
983  
984  
985  
986  
987  
988  
989  
990  
991  
992  
993  
994  
995  
996  
997  
998  
999  
1000

1  
2  
3  
4 Filatov, A. S.; Musaev, D. G.; Lewis, J. C. Mono-N-protected amino acid ligands  
5  
6  
7 stabilize dimeric palladium(II) complexes of importance to C–H functionalization. *Chem.*  
8  
9  
10 *Sci.* **2017**, *8*, 5746–5756.

11  
12  
13  
14 (28) Frisch, M. J.; Trucks, G. W.; Schlegel, H. B.; Scuseria, G. E.; Robb, M. A.;  
15  
16  
17  
18 Cheeseman, J. R.; Scalmani, G.; Barone, V.; Mennucci, B.; Petersson, G. A.; Nakatsuji,  
19  
20  
21 H.; Caricato, M.; Li, X.; Hratchian, H. P.; Izmaylov, A. F.; Bloino, J.; Zheng, G.;  
22  
23  
24  
25 Sonnenberg, J. L.; Hada, M.; Ehara, M.; Toyota, K.; Fukuda, R.; Hasegawa, J.; Ishida,  
26  
27  
28 M.; Nakajima, T.; Honda, Y.; Kitao, O.; Nakai, H.; Vreven, T.; Montgomery Jr., J. A.;  
29  
30  
31  
32 Peralta, J. E.; Ogliaro, F.; Bearpark, M.; Heyd, J. J.; Brothers, E.; Kudin, K. N.;  
33  
34  
35  
36 Staroverov, V. N.; Kobayashi, R.; Normand, J.; Raghavachari, K.; Rendell, A.; Burant, J.  
37  
38  
39 C.; Iyengar, S. S.; Tomasi, J.; Cossi, M.; Rega, N.; Millam, J. M.; Klene, M.; Knox, J. E.;  
40  
41  
42  
43 Cross, J. B.; Bakken, V.; Adamo, C.; Jaramillo, J.; Gomperts, R.; Stratmann, R. E.;  
44  
45  
46 Yazyev, O.; Austin, A. J.; Cammi, R.; Pomelli, C.; Ochterski, J. W.; Martin, R. L.;  
47  
48  
49  
50 Morokuma, K.; Zakrzewski, V. G.; Voth, G. A.; Salvador, P.; Dannenberg, J. J.;  
51  
52  
53  
54  
55  
56  
57  
58  
59  
60

1  
2  
3 Dapprich, S.; Daniels, A. D.; Farkas, Ö.; Foresman, J. B.; Ortiz, J. V; Cioslowski, J.;

4  
5  
6  
7 Fox, D. J. Gaussian 09, Revision D.01, Gaussian, Inc., Wallingford, CT, 2009.  
8  
9

10  
11 (29) Grimme, S.; Ehrlich, S.; Goerigk, L. Effect of the damping function in dispersion  
12 corrected density functional theory. *J. Comput. Chem.* **2011**, *32*, 1456–1465.  
13  
14  
15  
16  
17

18  
19 (30) Andrae, D.; Häussermann, U.; Dolg, M.; Stoll, H.; Preuss, H. Energy-adjusted ab  
20 initio pseudopotentials for the second and third row transition elements. *Theor. Chim.*  
21  
22  
23  
24  
25  
26 *Acta* **1990**, *77*, 123–141.  
27  
28

29 (31) Marenich, A. V.; Cramer, C. J.; Truhlar, G. D. Universal solvation model based on  
30  
31  
32  
33 solute electron density and a continuum model of the solvent defined by the bulk  
34  
35  
36 dielectric constant and atomic surface tensions. *J. Phys. Chem. B*, **2009**, *113*, 6378-  
37  
38  
39  
40 6396.  
41  
42  
43  
44  
45  
46  
47  
48  
49  
50  
51  
52  
53  
54  
55  
56  
57  
58  
59  
60